Energy 331 (2025) 136713

Contents lists available at ScienceDirect

Energy

journal homepage: www.elsevier.com/locate/energy

Future wave energy evolution in the Bay of Biscay for different converters

Hodei Ezpeleta [a,*], Alain Ulazia [a], Oihana Aristondo [b], Gabriel Ibarra-Berastegi [c,d]

[a] Department of Energy Engineering, University of the Basque Country (UPV/EHU). Engineering School of Gipuzkoa-Eibar, Spain
[b] Department of Applied Mathematics, University of the Basque Country (UPV/EHU). Engineering School of Gipuzkoa-Eibar, Spain
[c] Energy Engineering Department, University of the Basque Country (UPV/EHU), Alda. Urkijo, 48013 Bilbao, Spain
[d] Plentziako Itsas Estazioa, University of the Basque Country (UPV/EHU), Areatza Hiribidea 47, 48620 Plentzia, Spain

ARTICLE INFO

Keywords:
Wave energy
ERA5
CMIP6
Long-term energy trends
WEC

ABSTRACT

Future SSP5-85 IPCC scenario of Coupled Model Intercomparison Project 6 future projections (2015–2100) of wave data – significant wave height and wave peak period – are used to implement them in the power matrix of different wave energy converters: floating body, floating oscillating water column, and oyster device. An annual and seasonal study has been carried out in the nearest grid point to Mutriku's oscillating water column wave energy plant, a referential real wave energy converter integrated in a breakwater. Overall, the results show a negative trend evolution both in the Wave Energy Flux resource and in the production of the Wave Energy Converters. Because of their productive results, the Reference Model 3 and the Reference Model 5 wave energy converters have been selected for further production analysis. Most results have shown a downward trend both in the physical parameters and in the energy production of the wave energy converters and the wave energy flux. However, the future trends are not as strong as the past historical trends found in the North Atlantic in general, showing an inflection point in the climate change effects for marine energy environments. This inflection should be considered for possible smaller energy production, but this effect does not mean that there will be a relaxing of extreme energetic events.

1. Introduction

Within the reality of climate change, the decarbonization of the energy sector is a duty that humanity must take to reduce greenhouse gas (GHG) emissions and thus also reduce the environmental impact [1]. The ocean renewable energy (ORE) has the potential to reduce emissions due to its great flow that manifests itself in the form of wind, waves and tides, among others. The use of these resources could help achieve the European Union's (EU) 2050 decarbonization targets [2]. These specific targets are a 40% global reduction and a net domestic reduction of at least 55% in GHG emissions by 2030 compared to 1990, and 27% of total energy production from renewable energy sources [3]. Therefore, among OREs, less developed energy sources such as wave energy can play an important role in present and future electricity production apart from well-known technologies such as wind and solar [4]. The need for diversification in marine energy generation systems would change the current climate situation towards neutrality [5]. In this regard, hybrid approaches that integrate hydrokinetic energy with other renewables, such as photovoltaic and wind, have demonstrated their potential to enhance energy reliability and sustainability in isolated infrastructures, highlighting the importance of multi-source marine energy systems for the energy transition [6].

Although advances in Wave Energy Converters (WECs) still present challenges such as feasibility, durability and survivability in the face of extreme events, the synergy between wave energy farms [7] and coastal protection [8] in terms of mitigating the effects of global warming on the coastline, as for example in Mutriku, is a promising collateral innovation in favour of WECs. The mentioned synergy contains a fundamental aspect that requires long-term analysis of the resource under climate change scenarios. Another positive aspect in the development of WECs is the recent interest in assessing offshore wind and wave energy for combined renewable energy production [9], as hybrid approaches offer promising pathways for improving energy reliability and reducing costs [10]. Combined wind-wave energy systems can optimize energy capture by leveraging complementary resource profiles, where wind energy is generally more stable but wave energy provides a higher energy density per unit area [11]. Studies on the west Iberian nearshore indicate strong synergy between wind and wave power, making the development of joint wind-wave projects a viable option in high-resource coastal environments [12]. Moreover, site selection plays a crucial role in ensuring economic feasibility, with multi-criteria decision-making (MCDM) approaches identifying optimal

* Corresponding author.
E-mail address: hodei.ezpeleta@ehu.eus (H. Ezpeleta).

https://doi.org/10.1016/j.energy.2025.136713
Received 21 November 2024; Received in revised form 30 April 2025; Accepted 19 May 2025
Available online 5 June 2025

List of Abbreviations	
BBDB	Backward Bent Duct Buoy
BEM	Boundary Element Method
BIMEP	Biscay Marine Energy Platform
C3S	Copernicus Climate Change Service
CAES	Compressed Air Energy Storage
CI	Confidence Interval
CMIP 5 & 6	Coupled Model Intercomparison Project Phases 5 and 6
CSIRO	Commonwealth Scientific and Industrial Research Organisation
DOE	US Department of Energy
EU	European Union
ECMWF	European Centre for Medium-Range Weather Forecasts
EES	Energy Storage Systems
GHG	Greenhouse Gases
JPD	Joint Probability Distribution
LCOE	Levelized Cost of Energy
MBC	Multivariate Bias Correction of Climate Model Outputs
MHK	Marine Hidrokinetic
MPD	Model Predictive Control
NREL	National Renewable Energy Laboratory
OES	Ocean Energy Systems
ORE	Ocean Renewable Energy
ORNL	Oak Ridge National Laboratory
OSWEC	Ocillating Wave Energy Converter
OWC	Oscillating Water Column
OWSC	Oscillating Water Surge Converter
PNNL	PAcific Northwest National Laboratory
POEM	Plan de Ordenación del Espacio Marítimo
PTO	Power Take-Off
QMD	Quantile Mapping and Dressing
RM	Reference Model
RMP	Reference Model Project
SNL	Sandia National Laboratories
SSPs	Shared Socioeconomic Pathways
WEC	Wave Energy Converter
WEF	Wave Energy Flux
Nomenclature	
AEP	Annual Energy Production [kWh]
B	Capture width of WECs cavities [m]
CWR	Capture Width Ratio [%]
g	Earth's gravity force acceleration [9.81 m/s^2]
N	Number of analysed cases per year [2922 cases]
$P\left(H_{s_i}, T_{p_i}\right)$	Power based on WECs power matrices [kW]
P_{abs}	Power absorbed [kW]
P_{wave}	Wave power absorbed by WECs [kW]
T_e	Wave energy period [s]
T_m	Mean wave period [s]
T_p	Peak wave period [s]
Δt	Time period [3 h]
ρ	Water density [kg/m^3]
α	Wave periods relation ratio [-]

locations where wind and wave energy resources align with infrastructure accessibility and environmental constraints [13]. The integration of wave energy with floating wind platforms further enhances economic and operational efficiency by sharing mooring systems, power transmission infrastructure, and maintenance logistics, reducing overall capital and operational expenditures [11]. These hybrid systems not only improve energy output stability but also lower the levelized cost of energy (LCOE) over time compared to standalone wave farms, with recent studies highlighting that hybrid projects can reduce energy variability and enhance overall grid reliability [13]. As WEC technology continues to mature, its integration with other offshore renewable sources will be essential to making marine energy a competitive and reliable component of the global energy transition, especially considering that resource trends are evolving [12].

Several studies have already shown a general increase in wave height [14] and its energy worldwide [15] using past data and future projections via the Coupled Model Intercomparison Project Phases 5 and 6 (CMIP5 [16] and CMIP6 [17]). The effects of these historical increments on the energy production of different wave energy converters have also been analysed by some of the authors in Ireland [18], Chile [19], Iceland [20] or the Gulf of Biscay [21] using reanalysis data of ERA-20C (last century) calibrated against different reanalysis products.

Given these reasons, the present study focuses on the newest CMIP6 long-term wave period trends (2015-2100) at the nearest grid point from the Mutriku wave power plant and how it will affect different WECs with the aim of achieving an adequate projection of both Wave Energy Flux (WEF) and energy production. It will be done under the SSP5-85 scenario giving the option to compare it with the Mutriku oscillating water column (OWC) plant.

2. Data and methods

This section covers everything from the data set used for calibration to the methods used to analyse the data and obtain the results, as well as descriptions and characteristics of the WECs and the grid point.

2.1. Data

The data used here constitute a unique source for future CMIP6 projections incorporating wave data via an atmosphere-oceanic coupling simulation. According to the original methodology presented here, as it is shown in the next sections, these data about wave period and wave height are essential to obtain the instantaneous generation power of different WECs via their power matrices (Eq.-(4)). For further information about this section see the previous work of the authors (Ezpeleta et al. [22]).

2.1.1. Location

The grid point is located at coordinates 43.5° N, −2.5° W, in the southeastern Bay of Biscay (Fig. 1a). This location has been selected because it is the closest grid point to Mutriku in the dataset and this allows the possibility of future wave generation trends analysis between the present paper research and Mutriku's OWC wave plant. It should be noted that it is also the closest gridpoint to Biscay Marine Energy Platform (BIMEP), an area reserved for researching and testing different types of renewable ocean energy converters (Fig. 1c). So it is a well known area for its energy potential. It is necessary to emphasize that the Basque seabed tends to drop sharply just a few kilometres off the coast, consequently, the point investigated is located about 13 km north of the coast of Lekeitio and at a depth of about 125 m, beyond the prohibitive limit of 10 km imposed by the European Commission [23], and well within the technical limit of anchoring depth of 1000 m [24].

In fact, another of the objectives of this study is to test the hypothesis that the energy resource projections in the location analysed justify the installation of such floating wind devices, since this experimental location must be analysed in the context of the Spanish government's maritime spatial planning plan for the Iberian Peninsula (Cantabrian and Mediterranean), and the Canary Islands (POEM, Plan de Ordenación del Espacio Marítimo [25]), showing a strong potential in the Bay of Biscay, mainly in Galicia and Asturias [26], and having expanded a research and development area about ten kilometres northwest of the already known BIMEP area [27].

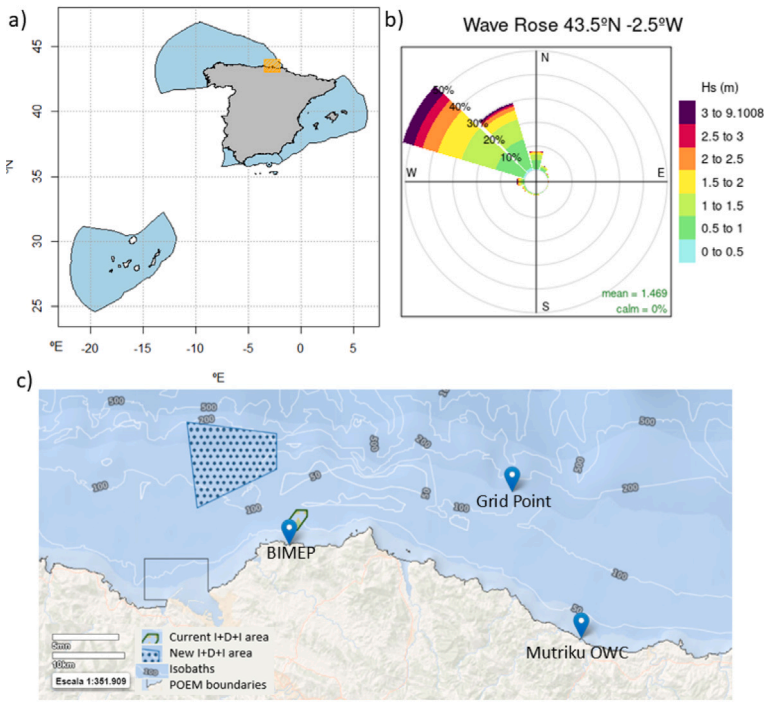

Fig. 1. (a) POEM, spanish government plan for maritime space management, establishes three main zones of important offshore wind energy potential: Bay of Biscay, West Mediterranean and Strait of Gibraltar, and Canary Islands. The studied area is coloured in orange. (b) Grid point wave rose. (c) Zoom of the studied area with the most relevant points [27]. (For interpretation of the references to colour in this figure legend, the reader is referred to the web version of this article.)

2.1.2. Reanalysis data

ERA5 reanalysis, the most advanced reanalysis of the European Centre for Medium-Range Weather Forecasts (ECMWF) and fifth major global reanalysis, has been used as a historical database and validation of future projections [28]. ECMWF processes all data sets using its IFS Earth System model (CY41R2) and the results are distributed by the Copernicus Climate Change Service (C3S) [29]. It covers the period from 1940 to the present and presents 1-hourly temporal resolution and a spatial grid of 30 km for the atmosphere, and 80 km for ocean wave where the parameters used in the present study are significant wave height (H_s) and wave peak period (T_p) [30]. Using these two parameters, the last tridecade (1985–2014) historical occurrence matrix is represented (Fig. 2) in order to compare it with the following 30-year periods of occurrence matrices analysed in the Section 3.

On the other hand, this historical database has been used also for the mean wave direction used for the wave-rose of [Fig. 1b]. This has been done to justify that the incident waves are mostly unidirectional and thus be able to use fixed WECs [See 2.1.6].

2.1.3. Future climate simulation data

The second data source used in this study is Commonwealth Scientific and Industrial Research Organisation (CSIRO), an ocean wave's climate simulations dataset [31]. The dataset has been globally validated against satellite altimeter and in situ buoy data, and when compared to traditional trend analyses, these models show that they can reproduce the main historical climate signals and produce statistically significant trends [32].

The dataset is obtained by coupling the WaveWatch III (v6.07) model with CMIP6 models. In the case of the present study, the model is run under the SSP5-85 IPCC Shared Socioeconomic Pathway and two models (ACCESS-CM2 and EC-EARTH3) with two parametrizations (CDFAC1, CDFAC1.08) for each one [33]. Therefore, there are four different future projections mixed under the highest-end forcing pathway scenario in terms of greenhouse gas emission (SSP5-85) [34].

The dataset contains 3-hourly outputs in a global 0.5° × 0.5° spatial resolution, in the 2015–2100 period, with an added historical period (1985–2014). The variables used in the study are peak wave period (T_p) and significant wave height (H_s). Therefore, due to the spatial resolution, the location and its surroundings share the same characteristics and comply with the legal limitations and technical limitations of the converters.

2.1.4. Calibration method

The CSIRO future projections were calibrated using ERA5 data to improve their accuracy. This calibration is necessary because the projections lack certain information that reanalysis data already has assimilated, such as meteorological ocean observations. For the present study, the variables T_p and H_s were selected and were corrected using Quantile Mapping and Dressing (QMD) function of the Multivariate Bias Correction of Climate Model Outputs (MBC) (R-package: https://CRAN.R-project.org/package=MBC) [35]. This methodology is particularly important for climate change research, since it allows for more accurate projections of future climate conditions [36]. Some of the authors have previously used this technique in studies related to wave [21] and wind energy [22] matching the quantiles in a direct way, e.g. [37].

2.1.5. WaveBot 5 & WaveBot 10 wave energy converters

The WaveBot devices have been modelled using the open-source boundary element method (BEM) solver NEMOH [38]. They are two similar WEC point absorber prototypes and the difference between them is the size. One has 5 m diameter and the other has 10 m diameter. In the Fig. 3 Wave Bots meshes and their Power Matrices can be seen.

Two prototypes of different sizes have been chosen because WaveBot 5 reaches nominal power, or goes into resonance, at relatively low periods compared to the grid point average. WaveBot 10, on the other hand, being larger in geometry, reaches resonance at longer periods because the natural frequency of a body increases as its mass decreases.

Every single WEC extracts its maximum energy when the system is at resonance, in other words, when the oscillating body velocity is in-phase with the hydrodynamic wave excitation force. It is therefore important to design the wave energy converter with a natural frequency that closely matches the dominant wave frequencies at the deployment site.

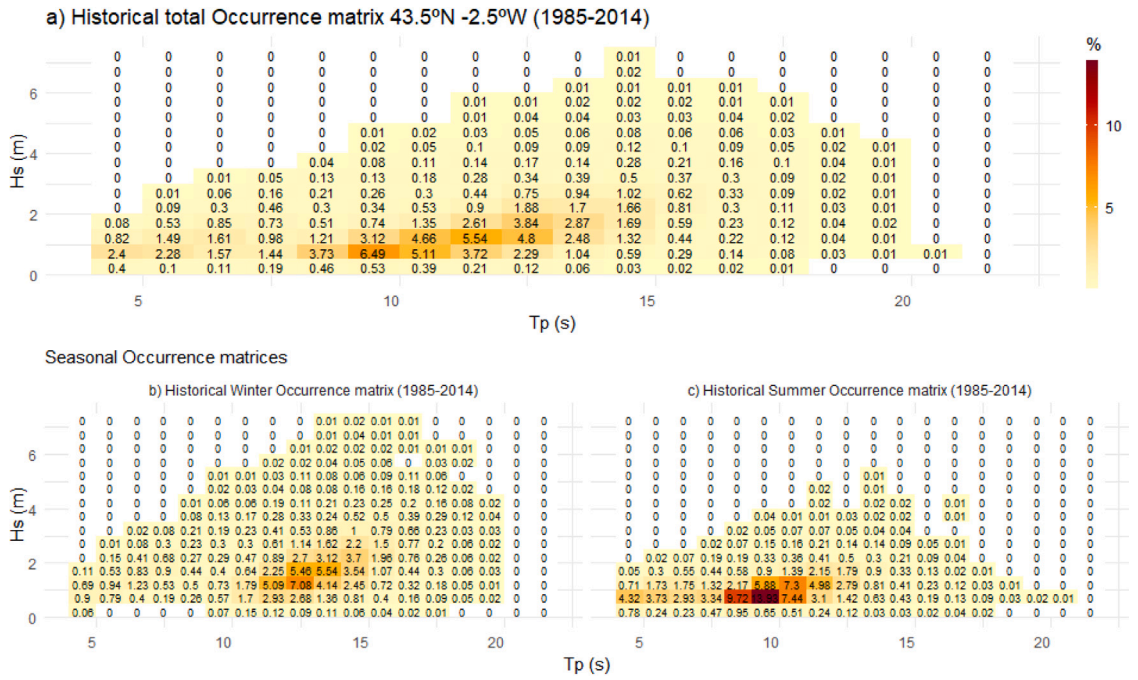

Fig. 2. (a) Gridpoint Historical total occurrence matrix (1985–2014) with its seasonal occurrence matrix (b) winter and (c) summer.

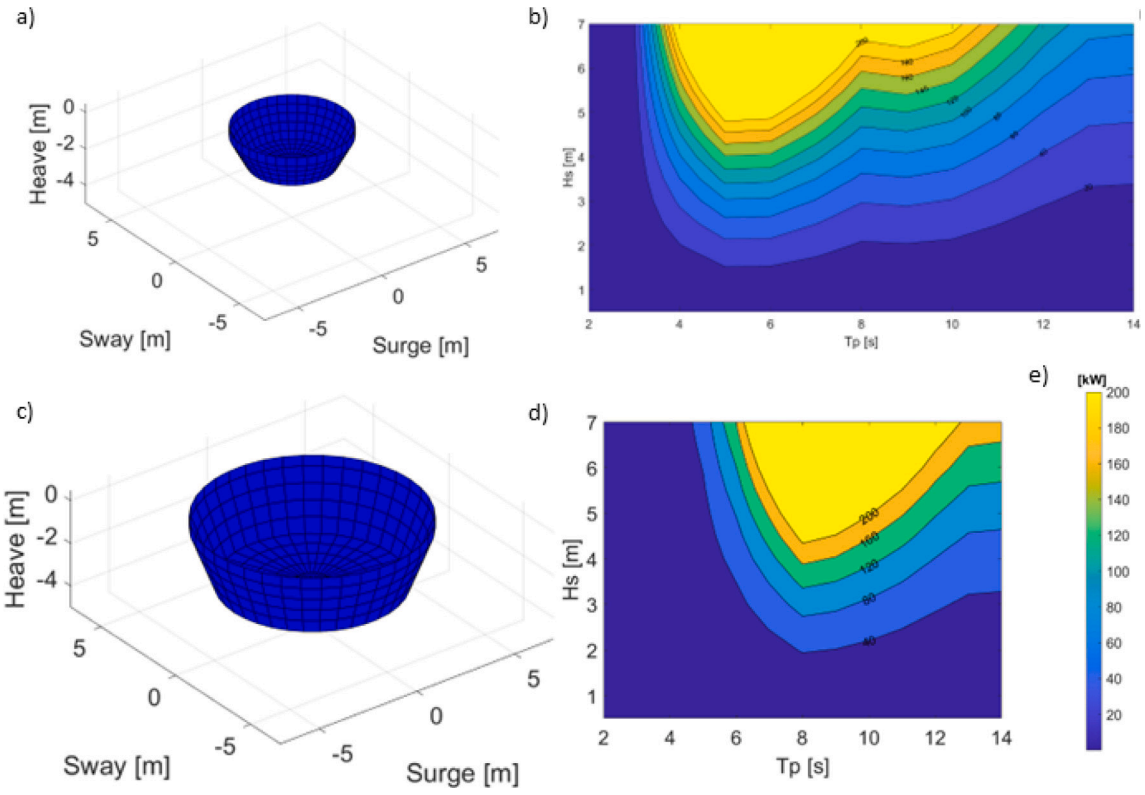

Fig. 3. (a) Mesh for the NEMOH based 5 m diameter WaveBot point absorber. (b) WaveBot 5 Power Matrix. (c) Mesh for the NEMOH based 10 m diameter WaveBot point absorber. (d) WaveBot 10 Power Matrix. (e) Power Matrixes legend.

2.1.6. Reference model project wave energy converters

Other WECs used in the research are among the Reference Model Project (RMP) converters. The project (2010–2014) was sponsored by the US Department of Energy (DOE) [39] and was a joint effort to develop open source marine hydrokinetic (MHK) point designs as reference models (RM) for comparing MHK technology performance and costs and an open source methodology for the design and analysis of MHK technologies, including models for estimating their capital costs, operating costs, and levelised costs of energy (LCOE) [40]. The RMP project team, led by Sandia National Laboratories (SNL) [41], included a partnership between DOE [39], three national laboratories, including the National Renewable Energy Laboratory (NREL) [42], Pacific

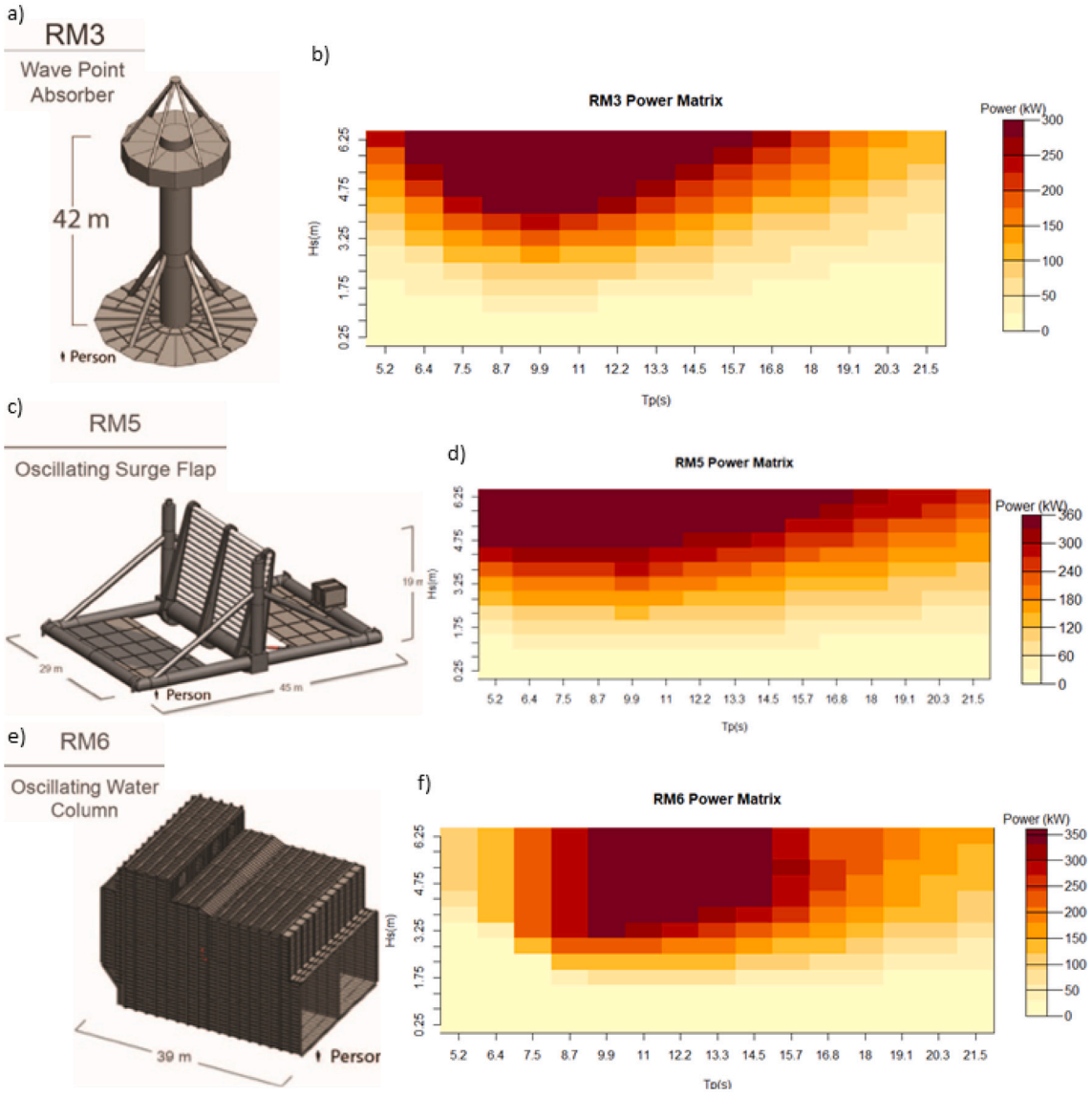

Fig. 4. (a) RM3 model size. (b) RM3 Power Matrix. (c) RM5 model size. (d) RM5 Power Matrix. (e) RM6 model size. (f) RM6 Power Matrix. [47].

Northwest National Laboratory (PNNL) [43] and Oak Ridge National Laboratory (ORNL) [44]. In addition, the Applied Research Laboratory at Penn State University [45] and Re Vision Consulting [46].

The Reference Model 3 (RM3) wave absorber is a floating heaving device. It was designed for a reference site off the coast of Eureka, Humboldt County, California. The device design consists of a surface float that oscillates with wave motion in relation to a vertical column buoy, which is connected to a subsurface reaction plate. The float is designed to oscillate up and down the vertical axis up to 4 m. The bottom of the reaction plate is about 35 m below the water surface. The device is designed to be deployed at depths up to 100 m. The point absorber is also connected to a mooring system to keep the floating device in position [48].

The Reference Model 5 (RM5) is a terminator type of Oscillating Wave Energy Converter (OSWEC) or Oscillating Wave Surge Converter (OWSC). The fin is designed to rotate against the support frame to convert wave energy into electrical energy. This study is focused on deep-water wave designs (50–100 m), where the device is tethered to the seafloor [49]. Because the grid point's site climate has a relatively stable NW wave direction for operational waves (Fig. 1b), the analysis presented in the study assumed unidirectional waves, and incident wave direction perpendicular to the surface of the OSWEC RM5 fin.

The Reference Model 6 (RM6) is a Backward Bent Duct Buoy (BBDB), which is a type of floating OWC wave energy converter [50]. The BBDB design consists of an airlock, an L-shaped duct, bow and stern buoyancy modules, and a power take-off (PTO) consisting of a Wells air turbine and a generator. The energy is produced by the movement of the wave, which varies the ambient pressure in the air chamber, thus forcing air flow through the Wells turbine. This design is intended to withstand hydrostatic pressure at a depth of up to 25 m [51]. Similar to RM5, the analysis assumes that the waves are unidirectional and perpendicular to the forward-facing float.

Given that these three models are reference models, they have been simulated and compared between them and the WaveBots under the objective of validating and obtaining the best option at the grid point.

2.2. Methods

The equations used to analyse the wave resource as well as the relationship between the parameters and the power matrix for the simulation of energy production are shown below.

Table 1
Main characteristics of the Fig. 3 WaveBot buoys.

Model	Diameter/Capture Width (m)	Cut off H_s (m)	Cut off T_p (m)	Rated Power (kW)	Resonance (T_p)
WaveBot 5	5	7	14	423	5–6
WaveBot 10	10	7	14	518.4	8

Table 2
Main characteristics of the Fig. 4 Reference Model WECs.

Model	Diameter/Capture Width (m)	Cut off H_s (m)	Cut off T_p (m)	Rated Power (kW)	Resonance (T_p)
RM3	20	6	21	286	9.0–10.0
RM5	25	6	21	360	9.0–10.0
RM6	27	6	21	350.5	9.5–10.5

2.2.1. Wave energy resource

For wave energy characterization, the WEF or the power per unit width of the wave crest is calculated. For WEF equation [Eq.-(1)], a deep water approximation is considered where the ratio between the water depth and the wavelength is bigger than $\frac{1}{2}$ as in the case of the present study's grid point [52].

$$WEF = \frac{\rho g^2}{64\pi} H_s^2 T_e = 0.49 H_s^2 T_e \tag{1}$$

WEF is the wave energy flux in kW/m Te is the wave energy period, ρ is the water density, and g is the acceleration of gravity. Based on this equation, more wave power is available when the wave height is larger and the wave period is longer [53].

It should be noted that mean wave period (T_m) is actually energy period (T_e) for ECWMF models and reanalysis for its approximation in deep waters for WEF [54].

$$T_m = T_e \tag{2}$$

On the other hand, the peak period T_p should be used for validation or implementation of the wave period in power matrices of different wave energy converters. Cahill et al. [53] defined a scaling factor (α) as a wave period ratio for the correction of different wave period definitions. Although this period scale correction is obviously not relevant for the calculation of the generation power presented here since the calculation is done directly by applying the power matrix to the direct projections, the factor will be calculated in order to make the results and matrices more visual and better interpretable under the same parameter (T_p) and so that in future works this correction value will be taken as a reference in the site and surroundings.

$$T_m = \alpha T_p \tag{3}$$

2.2.2. Annual energy production and capture width ratio

As the dataset used in the study has 3 hourly outputs, the δt will be 3 h and the number of data in a year will be $N = 365.25 \cdot (24/3) = 2922$ data. This will help to calculate the Annual Energy Production (AEP) [Eq.-(5)], and the Capture Width Ratio (CWR) [Eq.-(6)]. The first one [Eq.-(5)], is the total amount of electrical energy produced over a year; and the second one [Eq.-(6)] is the quantified power performance obtained by division between the power absorbed by the WEC and the total wave power arriving at the WEC, or in other words, is the ratio between the absorbed energy and the energy available in the wave front crossing the WEC [55].

$$P_{abs} = P\left(H_{s_i}, T_{p_i}\right) \tag{4}$$

$$AEP = \sum_{i=1}^{N} P\left(H_{s_i}, T_{p_i}\right) \cdot \Delta t \tag{5}$$

$$CWR = \frac{P_{abs}}{P_{wave}} = \frac{P_{abs}}{WEF \cdot B} \tag{6}$$

P(H_{s_i}, T_{p_i}) is the function that relates, using the power matrix, the produced power in function of the significant wave height and the peak period. Pabs is the power absorbed by the WEC and Pwave is the energy of the WEF multiplied by the capture width of the WEC cavity (B).

2.2.3. Future trend computation

Theil–Sen method has been used to compute the trends in values organized monthly. Additionally, WECs' performances are given in section [Results - 3.4] with boxplots and barplots of 30 and 10 years period changes respectively.

On the other hand, the wave statistics data are presented in terms of their joint probability distribution (JPD), or occurrence matrix, which indicates the probability of a significant wave height and wave energy period pair that occurs during a year for the reference resource.

3. Results

Given the importance of climatic patterns in the overall analysis, and to avoid that interference, this section shows wave data occurrence matrices and WECs performance-boxplots with 30-year period changes (tridecades) [56].

3.1. Data validation

The validation focused on the boxplot diagrams, which allow comparing different parameterizations and models with reference data (see 2.1.4) on the same graph. The results indicate similarity across the variables analysed T_p and H_s. The bias error [57] has been improved in all cases which are shown in the boxplots [Fig. 5] below. The boxplots contain diagrams in pairs of the same colour (non calibrated on the left, calibrated on the right) for each of the simulations including parametrization that take part in the final data mix analysed in this paper.

On the other hand, once the data have been calibrated and validated, the alpha value [Eq.-(3)] for the gridpoint has been obtained. For this purpose, the mean wave period (T_m) and peak wave period (T_p) variables have been compared historically (1985–2014) and this value has been applied to the future T_p variable for its conversion to T_m and future calculations.

The result has been that the alpha value is 0.798 as can be seen in the boxplot below [Fig. 6]. This value will be used in the location and its surroundings in future research.

3.2. Future wave trends

Future wave trends in the grid point are analysed through thirty year period occurrence matrices. For the climatological standards, tridecades as a reference period corresponds to the current guidelines by the World Meteorological Organization [58], or institutes such as the Copernicus Climate Change Service [59] because it helps smooth annual climate variations and allows teleconnection patterns of change to be identified over longer periods.

As can be seen in 2.1.2, [Fig. 2a], the hotpoint overall surrounds the occurrences of 10 s of T_p and 1 m of H_s in general. Analysing the difference between the historical data and the following three tridecades, the probability of occurrences of H_s-s less than one metre

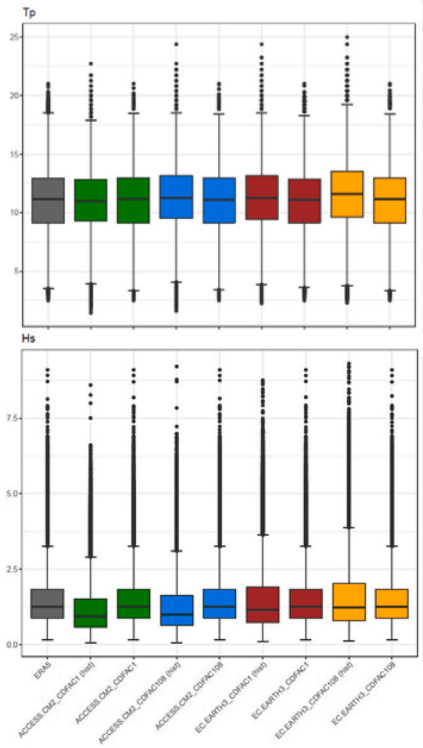

PARAMETER	SIMULATION	BIAS
T_p	historical_ACCESS.CM2_CDFAC1	0.07
	ACCESS.CM2_CDFAC1	0.00
	historical_ACCESS.CM2_CDFAC108	0.35
	ACCESS.CM2_CDFAC108	0.00
	historical_EC.EARTH3_CDFAC1	0.34
	EC.EARTH3_CDFAC1	0.00
	historical_EC.EARTH3_CDFAC108	0.62
	EC.EARTH3_CDFAC108	0.00
H_s	historical_ACCESS.CM2_CDFAC1	-0.30
	ACCESS.CM2_CDFAC1	0.00
	historical_ACCESS.CM2_CDFAC108	-0.22
	ACCESS.CM2_CDFAC108	0.00
	historical_EC.EARTH3_CDFAC1	-0.01
	EC.EARTH3_CDFAC1	0.00
	historical_EC.EARTH3_CDFAC108	0.09
	EC.EARTH3_CDFAC108	0.00

Fig. 5. T_p and H_s BIAS correction boxplots (left) and its correction values tables (right).

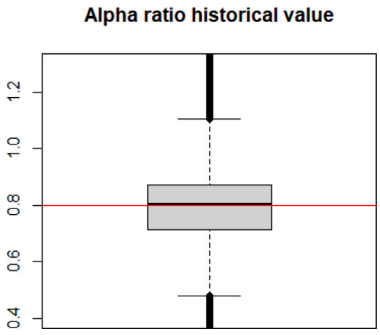

Fig. 6. Alpha's historical values boxplot.

increases and with respect to the T_p, apart from the fact that the hotpoint is maintained, shorter period occurrences increase.

Analysing the occurrence probability throughout the most relevant seasons composed by winter (January, February, March) and summer (July, August, September), with historical occurrences [Fig. 2b,c], next graphics are obtained [Fig. 8]:

It seems that the same phenomenon of the total occurrences cases [Fig. 7] is repeated also in the seasonal occurrence changes [Fig. 8]. As it can be seen, the biggest changes occur in summer, exactly in waves smaller than 2 m and peak periods of around 10 s. The waves of around 2 m decrease and waves of around 1 m height increase. The same occurs in winter, but on a smaller scale.

Overall the main tendency of waves is to decrease, as well as the period. To convert this information into energy-trends terms, first WEF is calculated (Eq.-(1)) and the occurrence matrices are used to extract the instantaneous generation values.

3.3. Future wave energy production trends

The following table [Table 3] shows the future trends in a 95% of Confidence Interval (CI) and in the future SSP5-85 IPCC scenario of the WEF and the different WECs described in [WaveBot 5 & WaveBot 10 WECs 1 and Reference Model Project WECs 2], in general and in the most influential seasons, applying Theil–Sen method to each of the future values set. In other words, monthly dataset are evaluated with its quantile 2.5%, 50% and 97.5% and to the resulting three ranges – least powerful events (2.5% quantile), mean events (50% quantile) and most powerful events (97.5% quantile) – the Theil–Sen method is applied. To ensure that the Theil–Sen trend values to these three ranges CI are relevant, another 95% CI will be applied to each of the trends (top, median and bottom) making sure that if the Theil–Sen extreme values have the same sign, the value of the average ramp will be relevant. So that the general trends as well as the extreme trends in each of the cases can be deduced more accurately.

The WECs with the most relevant trends and the one with the most % of its rated generation power are chosen for deeper analysis as well as raw wave energy potential, the WEF.

The WEF trend is negative almost every single time. Mostly in summer, where its extreme events are supposed to descend by more than 2 kW/m per decade. This is related with the evolution of occurrence matrices [Figures-7,8] where the H_s decreases as well as the T_p and consequently, the T_m. Its mean values are also related with its historical (1985–2014) mean values, so the results obtained are under the same scale.

The main power trends are descending as well. There is no relevant increasing generation power trend and despite the fact that in both of the Wave Bot cases the no generation trends do not match with the power trends, probably because they are not significant, but the negative evolution of the power generation in RM project WECs and the positive trend in the no generation time make sense. On the other hand, as expected, winter is the most productive season and summer the least one making the WECs almost useless.

To further analysis, apart from WEF, RM3 and RM5 WECs are selected because their mean power generation has the highest values and they have little non-generation time. Otherwise, although Wave Bots are the ones which are practically producing all the time, its generation power is too little and it is because they are designed for

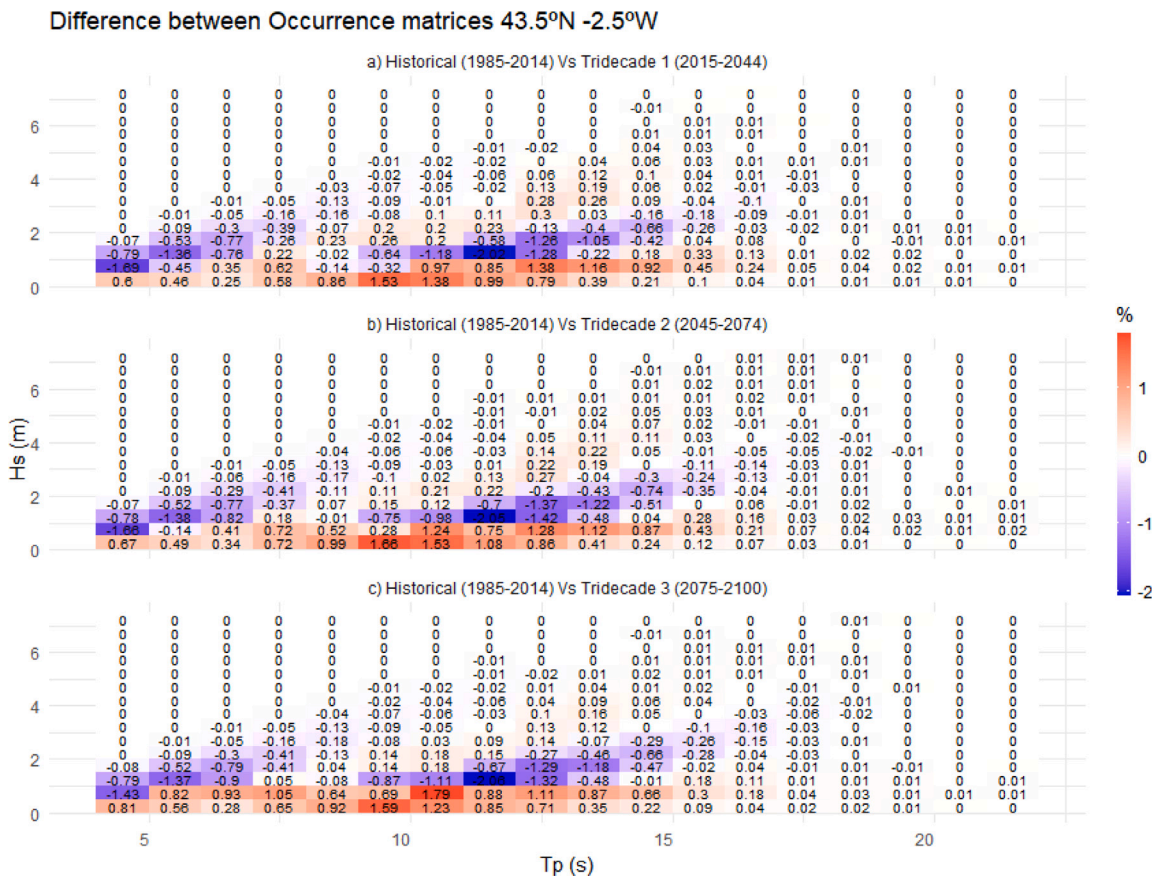

Fig. 7. Difference between Historical total [Fig. 2a] and (a) Tridecade 1 total occurrence matrix (b) Tridecade 2 total occurrence matrix and (c) Tridecade 3 total occurrence matrix.

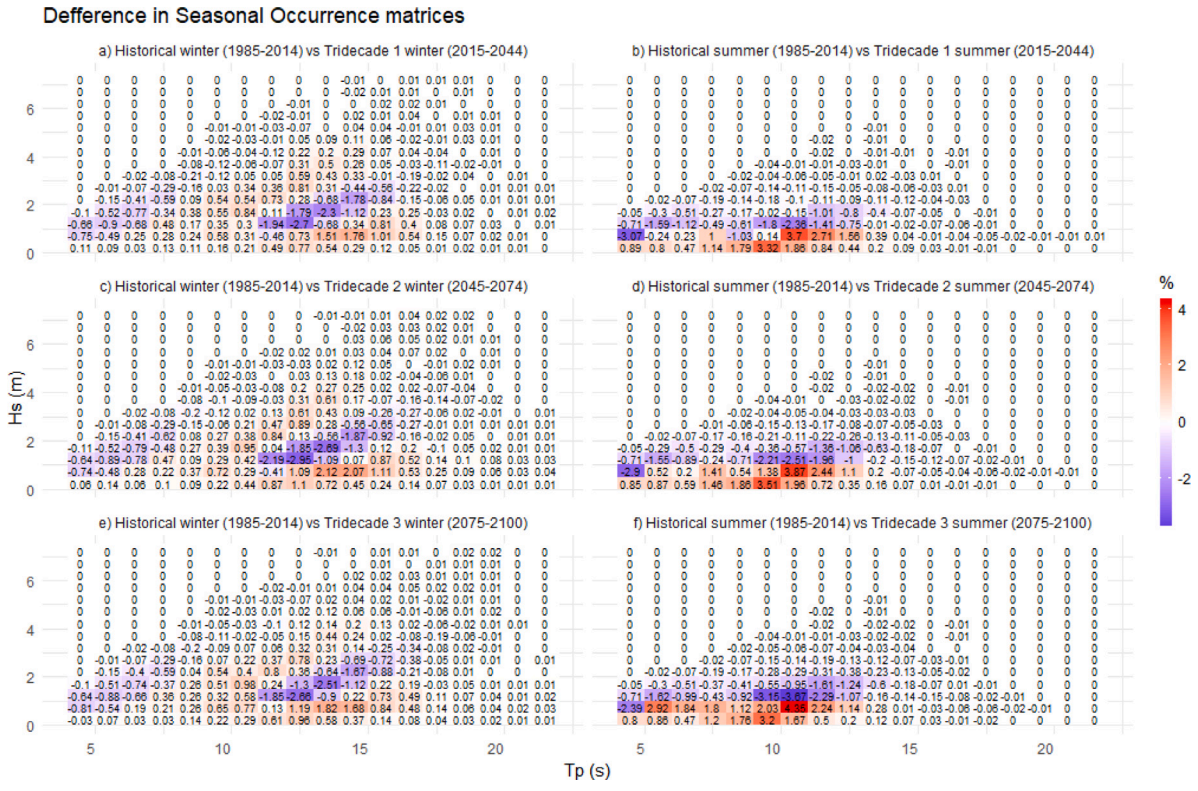

Fig. 8. Difference between Historical seasonal [Fig. 2b,c] and (a) Tridecade 1 winter occurrence matrix (b) Tridecade 1 summer occurrence matrix (c) Tridecade 2 winter occurrence matrix (d) Tridecade 2 summer occurrence matrix (e) Tridecade 3 winter occurrence matrix (f) Tridecade 3 summer occurrence matrix.

Table 3
Summary of the WEF power and WECs mean generation power trends.

Time period	Overall (2015–2100)						
Parameter	Bottom Confidence Interval slope (2.5%)	Central value slope	Top Confidence Interval slope (97.5%)	Mean value	% of Rated Power	% of time out of power generation boundaries	– No generation– trend (%/decade)
WEF (kW/m/decade)	−0.0050	−0.0788	−0.6513	13.03	–	–	–
WEF summer	0.0225	−0.1610	−2.7453	3.28	–	–	–
WEF winter	−0.0055*	−0.0098*	−4.3719*	24.18	–	–	–
WB5 (kW/decade)	0.0024	−0.0618	−0.1552	6.50	1.54%	0.02%	0.0002*
WB5 summer	0.0210	−0.2763	−1.0397	3.29	0.78%	0.01%	−0.0026*
WB5 winter	−0.0376*	−0.1971*	0.1748*	9.73	2.30%	0.01%	−0.0123
WB10 (kW/decade)	−0.0066	−0.1471	−0.4809	12.77	2.46%	0.15%	−0.0016*
WB10 summer	−0.0606	−0.7981	−4.0180	5.68	1.10%	0.10%	−0.0229
WB10 winter	−0.0621*	−0.3573*	0.3270*	19.99	3.86%	0.08%	−0.0406
RM3 (kW/decade)	−0.0057	−0.3734	−0.1010	33.87	11.84%	1.92%	0.0633
RM3 summer	−0.1027	−1.8581	−4.1467	12.37	4.32%	3.16%	0.4491
RM3 winter	−0.1591*	−0.9800*	1.9493*	55.73	19.49%	0.29%	−0.0864
RM5 (kW/decade)	−0.1101	−0.5413	−0.4490	57.27	15.91%	1.92%	0.0633
RM5 summer	−0.9305	−2.7987	−6.7636	28.28	7.86%	3.16%	0.4491
RM5 winter	−0.1867*	−1.0312*	1.5609*	86.26	23.96%	0.29%	−0.0864
RM6 (kW/decade)	−0.0019	−0.4372	−3.0937	45.87	13.09%	54.13%	0.4759
RM6 summer	0.00	−2.0215	−10.94	5.84	1.67%	83.61%	3.5668
RM6 winter	−0.1734	−1.7504*	0.4857*	87.55	24.98%	27.48%	0.4952*

* means that the slope is not relevant at a 95% confidence level.

an environment with smaller periods. Finally the RM6 is most of the time out of production. It has the ability to produce the most, as it can be seen in its winter mean generation power value, but it is not worthy given its high cost in operation and maintenance while floating and the risk that the moorings would break the huge floating OWC structure. For that it is better, and more real, to take Mutriku's OWC for future comparisons.

3.4. Future capture width ratio and annual energy production evolution

The figure below [Fig. 9] shows the changes throughout the different tridecades and the most relevant seasons of the WEF [Fig. 9a,b,c], RM3's CWR [Fig. 9d,e,f] and RM5's CWR [Fig. 9g,h,i]:

Starting with the WEF, excepting the summer, the historical values are similar to the following tridecades values. In addition, it shows the slightly negative trends also analysed in [Table 3]. In winter, it looks like the extremest events will increase in the first tridecade to start descending the following ones, but, overall and mainly in summer, the extremest values will decrease as time goes by.

With the two WECs, RM3 and RM5, at first sight, the changes are almost imperceptible. CWR graphics reflect the fraction of wave power flowing through the device that is absorbed by the device [55]. It looks like the CWR is much better in summer than in winter. In other words, in summer the WECs have more effective wave power absorption, since the natural wave energy available reduces more than the absorbed energy in the ratio of CWR.

Regarding values, the RM3's overall CWR is around 17% and the RM5's values are about 35%. These values are similar to the review research made by Babarit (2015) [55]. Here RM3 WEC obtained an annual average CWR of 16% [48], and RM5 an average CWR of 31% [60], both with the same size as analysed in this paper.

On the other hand, the next barplots [Fig. 10] show the decadal mean AEP of each WEC and the decadal mean annual available WEF under the same AEP term. The amount of those AEPs produced at each of the most influential stations are also shown.

As can be seen in the three bar charts [Fig. 10a,b,c], the AEP is slightly decreasing decade by decade. The last decade in particular is energetically poor compared to the others. Around 20% of production is lost in each of the simulations with respect to the historical AEP. This may be due to the fact that the last period of time consists of only 5 years and has not given time to regulate the production so that the average AEP would end up being similar to the others.

On the other hand, the winter energy input remains the most constant variable in all three graphs. Winter production varies between 40%–50% of the total WEF; between 35%–42% in RM3 AEP; and between 34%–40% in RM5 AEP. Although it can be seen that energy production gradually decreases, as also shown in Table-3, there are decades, such as decade 6, where the AEP decreases by 9% in the WEF, 13% in RM3 and 14% in RM5, but the average winter contribution increases by 7% and 4% respectively for the first two, and only decreases by 0.8% for RM5.

As for the average summer contribution, it is around 5%–10% of the total AEP for WEF; 7%–13% for RM3; and 10%–15% for RM5. As these values are much smaller than the rest, the negative trend greatly affects their absolute energy contribution, being reduced, in the penultimate decade (Decade 8), by up to 50% (−49% in the WEF, −45% in RM3, and −35% in RM5) with respect to the historical summer contribution. This is not the case of winter production, since that same decade (Decade 8) in the case of the WEF contributes 6% more, in the RM3 another 6% more and in RM5 it contributes almost 2% more than the historical contribution.

4. Discussion

From the experience of evaluating the economic impact of future trend as made in the previous work by the authors with offshore wind turbine [22], it is shown the difficulty to estimate in a global or standard base the WECs' LCOE. There are a lot of prototypes harvesting wave energy throughout different principles (Point Absorbers, Oscillating Wave Columns, Oscillating Wave Surge Converters, Terminator types, Fixed or Floating ones...) and although there are arising big projects as the AW-Energy WaveRoller WaveFarm [61] or the Carnegie Clean Energy's CETO project [62], the reality is that the magnitude and the type of each project depends on the marine environment location; even if there are areas of research and development to test different prototypes and models, such as BIMEP [63], Wave Hub [64] and The European Marine Energy Centre [65] among others, there are still no WEC farms on an industrial, commercial or utility scale as such, excepting the fixed OWC of Mutriku's port [66] which is the first and only wave energy project connected to the electricity grid in Europe still producing nowadays [67]. Given this reason, the LCOEs of the two Reference Models selected for the results (RM3 and RM5) are in an approximated way. In other words, as the models selected and

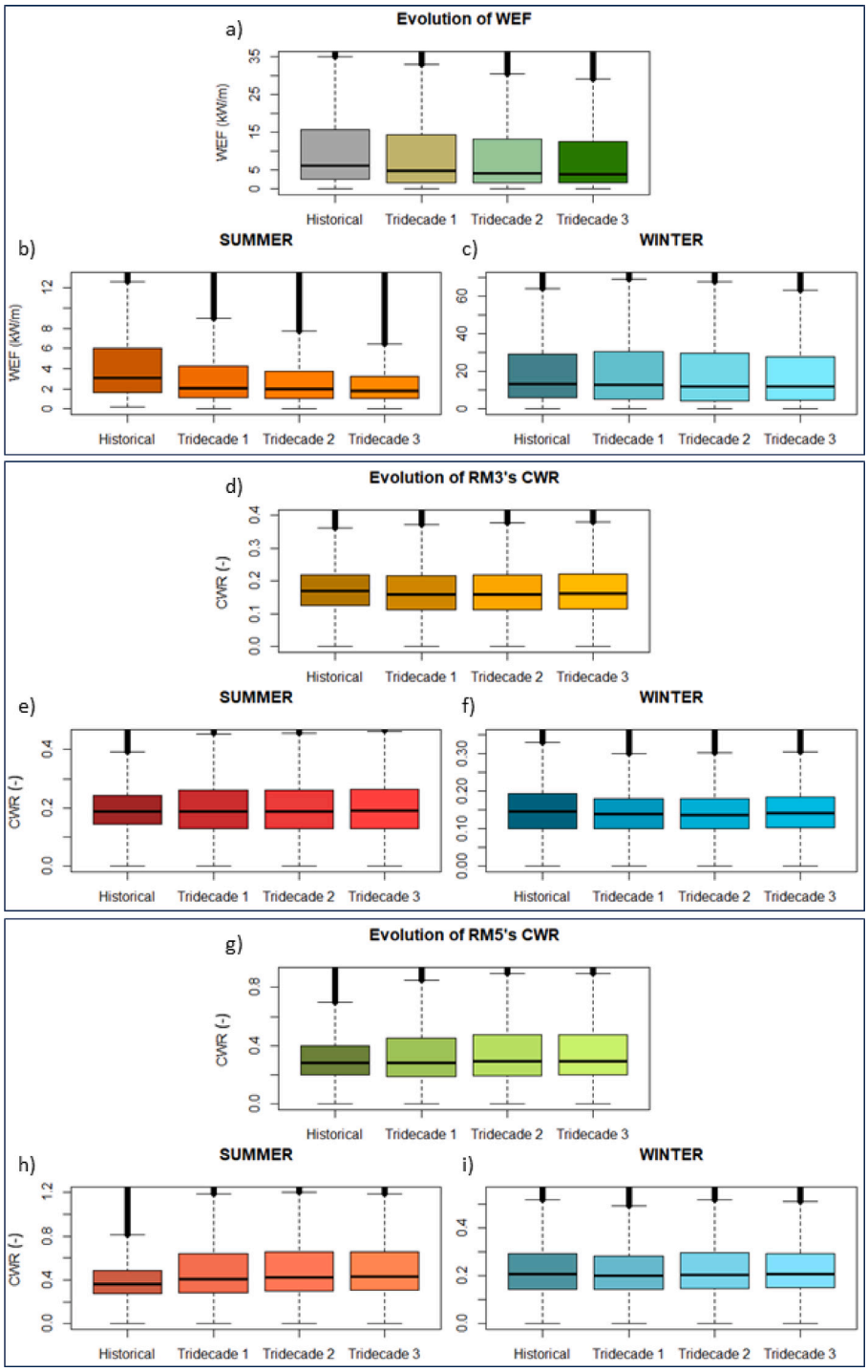

Fig. 9. Evolution of WEF [a,b,c], and RM3's [d,e,f] and RM5's [g,h,i] CWR throughout tridecades and most influential seasons [Summer and Winter].

simulated are reference models, corresponding LCOE will be referential as well.

According to NREL in 2015 [68], just when the future projection dataset starts (see 2.1.3), the RM3's LCOE vary between 1.41$/kWh in a 10 units array to approximately 0.73$/kWh for an array of 100 units in Humboldt Bay surroundings (California), and for RM5, between 1.44$/kWh in a 10 units array to approximately 0.69$/kWh for 100 units array in same location [69]. Since no grid-connected park of these converters has been launched yet and because the seabed of the simulated environment (see 2.1.1) is irregular and very steep, which means it does not allow mega-projects, the LCOE of the 10-unit array will be taken as a model for the economic estimation. Taking into account that the Euro/Dollar average exchange rate of 2015 was 1€=1.11$, the reference LCOE is 1.28€/kWh for RM3 and 1.32€/kWh for RM5.

The first years the RM3 would produce around 400,000€/year and RM5 bit less than 700,000€/year, of which ≈40% of the income would be made in winter and ≈10% in summer for the RM3 and the relation would be 37%/14% for the RM5. Maintaining the LCOE value table by 2100 as well as considering no inflation, with the negative production trends shown in results (see Table 3), this century's last years the production would drop to 350,000€/year for the RM3 and a bit more than 600,000€/year for the RM5. This means that in RM3's case, the production would decrease more than 12%, of which 42%

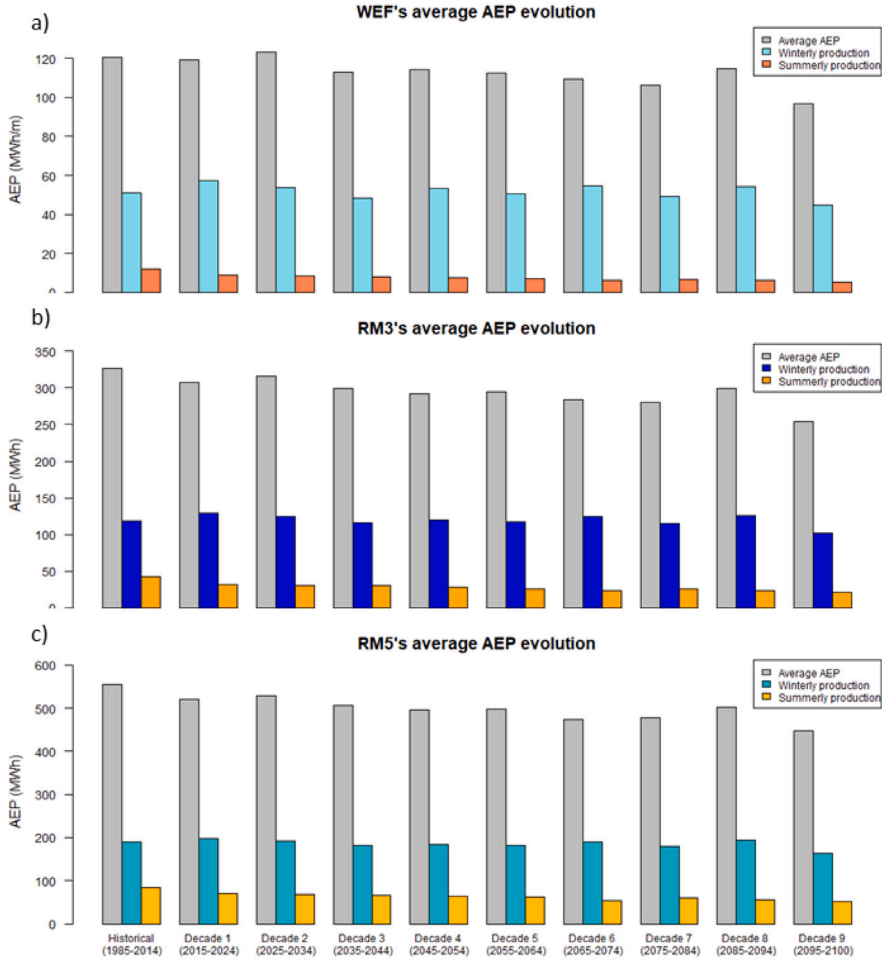

Fig. 10. Evolution of the AEP during different decades along with the evolution of winter and summer production in (a) WEF. (b) RM3. (c) RM5.

would be given in winter (falling around 8% from the first years' winter production) and 8% in summer (falling 30% from its first years' production); and in the RM5's case the decrease would be ≈12%, of which 38% of the production would be in winter (12% less than first years' winter production) and 11% in summer (more than 30% less than first years' summer production). This means that despite all the negative trends, even in winter and summer seasons, the relative value of the winter contribution in yearly production would increase and, otherwise, the summer contribution would decrease.

Looking ahead, WECs LCOE is expected to decrease significantly as the technology matures. According to NREL, wave energy's LCOE could drop to 0.30$/kWh by 2033 and potentially reach 0.07$/kWh by 2050 under optimistic scenarios, driven by advancements in structural design, operational efficiencies, and economies of scale [70]; M. deCastro et al. [71] evaluated the economic feasibility of wave energy along the Galician coast, a region with a similar resource profile to the Basque coast but with a less steep seabed, and found that WECs such as Atargis (in deep waters), Oyster (in shallow waters), and Wave Dragon (in shallow waters) could achieve LCOE values as low as 77-50-97€/MWh respectively, with an average of 70€/MWh for a wave farm in that environment. Notably, the RM5 device, the same model analysed in this study, emerged as one of the most cost-effective options, with projected LCOE values between 89–140€/MWh, marking almost a tenfold reduction from the 1.32€/kWh estimated a decade ago [49]. Further reinforcing this trend, the Ocean Energy Systems (OES) report [72] and IRENA projections [73] indicate that with continued technological progress and increased deployment, wave energy costs could align with offshore wind by 2035, reaching 100€/MWh. While wave energy still faces economic challenges due to its early-stage development, ongoing improvements in mooring systems, device performance, and large-scale deployment strategies are expected to drive substantial cost reductions [74], positioning it as a viable contributor to the future renewable energy mix [75].

However, beyond cost reductions, ensuring a stable energy supply despite declining production trends requires additional mitigation strategies. One such approach is optimizing WEC control to enhance power capture efficiency. Advanced control techniques, including optimal, robust, and nonlinear strategies, have been demonstrated to significantly improve energy extraction by adapting the device's resonance characteristics to varying wave conditions: a judicious control implementation can multiply the energy captured by a factor of two to four while maintaining system reliability and avoiding excessive loads that could lead to structural failures [76], and model predictive control (MPC) and direct transcription methods provide effective real-time energy maximization solutions for WECs, overcoming computational complexity issues associated with traditional optimization techniques [77].

Another crucial strategy is integrating energy storage systems (ESS) to counteract the intermittency of wave energy and ensure a reliable supply, particularly in isolated infrastructures and high-energy offshore environments. Arellano-Prieto et al. [78] identify promising offshore storage solutions, including compressed air energy storage (CAES), flywheels, and battery technologies, which can stabilize wave energy output and enhance grid integration. Additionally, hybrid wind-wave farms incorporating ESS, show that such configurations significantly reduce the storage capacity required while maintaining a stable power

supply [79]. These hybrid systems leverage the complementary nature of wind and wave energy, minimizing fluctuations and improving dispatchability. A particularly promising advancement in offshore storage is the Ocean Battery, a novel pumped hydro energy storage (PHS) system designed for seabed deployment. Unlike conventional PHS, this system operates in a closed hydraulic loop, minimizing environmental impact while achieving a round-trip efficiency of 77%, comparable to traditional onshore hydro storage [80]. Its integration into marine energy farms could offer a scalable, high-capacity storage solution that can store excess wave and wind energy and release it on demand, improving grid reliability and reducing curtailment losses.

Given the potential of these control and storage strategies, their implementation in future wave energy projects will be critical to ensuring economic viability and securing a stable contribution to the renewable energy mix.

5. Conclusions

The results confirm what other papers have already shown: the expected negative trends in the north Atlantic and Bay of Biscay in the parameters analysed for future decades [81] and its impact in power generation [22]; Sometimes due to the lack of energetic periods, and other times due to the surpass of offsets boundaries. The most uncertain season is winter, although the no generation time trends are significant and in most cases negatives. This means that the cases which were out of the offset boundaries, as time passes and the trend of the variables decreases, enter within the limits of the offset making less non generation time, but analogously, less overall power generation.

These negative results mean that we are in an inflection period passing from very strong positive trends to null or even negative trends according to historical studies of some of the authors coherent with other well known publications in different location as Iceland [20], Bay of Biscay [21], North-East Atlantic Ocean [37] and Mutriku [82]. The climatic and physical explanation of this phenomenon is out of scope of this paper, although it seems that there is a type of saturation in the kinetic energy absorption of the earth [22].

Another aspect to analyse is which WEC could perform better in this environment. According to the obtained results, the most suitable WEC would be the RM5. This type of OWSC, is the best option in environments in which there is a very clear trend of mean wave direction, as in this case. These types of OWSCs usually have the best performance of all as reported in [55]. But it should be noted that a floating heaving device, f.i. RM3, is easier to install and maintain, and performs better in areas where there is no predominant wave direction.

Comparing the losses with offshore wind energy potential, the previous work by the authors [22] shows that, in the same region, by 2100 the AEP of a 15MW offshore wind turbine will decrease by approximately 7%, with winter, the most productive season, experiencing a reduction of around 4%. Translating this into economic impact, the LCOE currently exceeds 0.16€/kWh on the West Cantabrian Coast, regardless of the floating and anchoring method, according to [83]. The IEA 15MW offshore wind turbine would see its annual generation reduced by 300,000–350,000€, and during winter, by 100,000–200,000€.

While these numbers highlight that both offshore wind and wave energy are subject to declining production trends, it is important to acknowledge that the LCOE of WECs remains significantly higher than that of offshore wind turbines. This discrepancy is largely due to the maturity gap between the two technologies. Offshore wind energy has undergone substantial technological advancements and cost reductions over the past decades, whereas wave energy is still in an early stage of commercial deployment. Consequently, direct economic comparisons should focus not solely on absolute LCOE values, but rather on the percentage of energy production losses over time. In this regard, the results indicate that wave energy is slightly more affected by long-term negative production trends than offshore wind, reinforcing the need for further technological development and cost reduction strategies in the wave energy sector.

Finally, given the universal nature of the presented methods, it would be possible to perform the same analysis in other marine regions around the world to analyse the wave energy potential future evolution and its energetic production following the previous work of the authors [84]. This research line will certainly contribute to a better design of future tentative wave farms that during their lifespan will have to face changes in the available oceanic potential. The current approach will contribute to more accurate feasibility studies. A better identification of the most appropriate WEC and how it will perform long-term in a wave farm will provide a more confident estimation of costs. This will attract more investors and stakeholders to give steps forward towards a further development of clean energy from waves.

CRediT authorship contribution statement

Hodei Ezpeleta: Writing – review & editing, Writing – original draft, Visualization, Validation, Supervision, Methodology, Investigation, Formal analysis, Data curation, Conceptualization. **Alain Ulazia:** Writing – review & editing, Writing – original draft, Supervision, Project administration, Investigation, Funding acquisition, Formal analysis, Conceptualization. **Oihana Aristondo:** Writing – review & editing, Writing – original draft, Supervision, Methodology, Investigation, Formal analysis, Conceptualization. **Gabriel Ibarra-Berastegi:** Writing – review & editing, Writing – original draft, Visualization, Validation, Supervision, Resources, Methodology, Investigation, Conceptualization.

Declaration of competing interest

The authors declare that they have no known competing financial interests or personal relationships that could have appeared to influence the work reported in this paper.

Acknowledgements

This study is part of project PID2020-116153RB-I00 funded by Ministerio de Ciencia e Innovación/Agencia Estatal de Investigación MCIN/AEI/ 10.13039/501100011033, and of the Grant PID2019-107539GB-I00 funded by Spanish Ministerio de Economía y Competitividad. The authors also acknowledge funding from the University of the Basque Country through PIF23/09 UPV/EHU formation grant and the Basque Government for research support (IT1694-22).

Data availability

Data will be made available on request.

References

[1] (IRENA) IREA. Renewable energy: A key climate solution. 2017, URL: https://www.irena.org/-/media/Files/IRENA/Agency/Publication/2017/Nov/IRENA_A_key_climate_solution_2017.pdf. [Accessed 5 November 2024].
[2] Council of the European Union. Climate change policy. 2024, URL: https://www.consilium.europa.eu/en/policies/climate-change/. [Accessed 5 November 2024].
[3] Colmenar-Santos A, Perera-Perez J, Borge-Diez D, dePalacio Rodríguez C. Offshore wind energy: A review of the current status, challenges and future development in Spain. Renew Sustain Energy Rev 2016;64:1–18.
[4] Weiss CV, Guanche R, Ondiviela B, Castellanos OF, Juanes J. Marine renewable energy potential: A global perspective for offshore wind and wave exploitation. Energy Convers Manage 2018;177:43–54.
[5] Görmüş T, Aydoğan B, Ayat B. Offshore wind power potential analysis for different wind turbines in the Mediterranean Region, 1959–2020. Energy Convers Manage 2022;274:116470.
[6] Icaza-Alvarez D, Jurado F, Tostado-Véliz M, Arevalo P. Design to include a wind turbine and socio-techno-economic analysis of an isolated airplane-type organic building based on a photovoltaic/hydrokinetic/battery. Energy Convers Manag: X 2022;14:100202.

[7] Clemente D, Rosa-Santos P, Taveira-Pinto F. On the potential synergies and applications of wave energy converters: A review. Renew Sustain Energy Rev 2021;135:110162.

[8] Abanades J, Greaves D, Iglesias G. Coastal defence through wave farms. Coast Eng 2014;91:299–307.

[9] Pérez-Collazo C, Greaves D, Iglesias G. A review of combined wave and offshore wind energy. Renew Sustain Energy Rev 2015;42:141–53.

[10] Kalogeri C, Galanis G, Spyrou C, Diamantis D, Baladima F, Koukoula M, Kallos G. Assessing the European offshore wind and wave energy resource for combined exploitation. Renew Energy 2017;101:244–64.

[11] Wan L, Moan T, Gao Z, Shi W. A review on the technical development of combined wind and wave energy conversion systems. Energy 2024;130885.

[12] Rusu L. An evaluation of the synergy between the wave and wind energy along the west Iberian nearshore. Energy Convers Manag: X 2023;20:100453.

[13] Hosseinzadeh S, Etemad-Shahidi A, Stewart RA. Site selection of combined offshore wind and wave energy farms: a systematic review. Energies 2023;16(4):2074.

[14] Lobeto H, Menendez M, Losada IJ. Future behavior of wind wave extremes due to climate change. Sci Rep 2021;11(1):7869.

[15] Reguero BG, Losada IJ, Méndez FJ. A recent increase in global wave power as a consequence of oceanic warming. Nat Commun 2019;10(1):1–14.

[16] Odériz I, Mori N, Shimura T, Webb A, Silva R, Mortlock T. Transitional wave climate regions on continental and polar coasts in a warming world. Nat Clim Chang 2022;12(7):662–71.

[17] Meucci A, Young IR, Trenham C, Hemer M. An 8-model ensemble of CMIP6-derived ocean surface wave climate. Sci Data 2024;11(1):100.

[18] Penalba M, Ulazia A, Ibarra-Berastegui G, Ringwood J, Sáenz J. Wave energy resource variation off the west coast of Ireland and its impact on realistic wave energy converters' power absorption. Appl Energy 2018;224:205–19.

[19] Ulazia A, Penalba M, Rabanal A, Ibarra-Berastegi G, Ringwood J, Sáenz J. Historical evolution of the wave resource and energy production off the chilean coast over the 20th century. Energies 2018;11(9):2289.

[20] Penalba M, Ulazia A, Saénz J, Ringwood JV. Impact of long-term resource variations on wave energy Farms: The Icelandic case. Energy 2020;192:116609.

[21] Ulazia A, Penalba M, Ibarra-Berastegui G, Ringwood J, Saénz J. Wave energy trends over the Bay of Biscay and the consequences for wave energy converters. Energy 2017;141:624–34.

[22] Ezpeleta H, Ulazia A, Ibarra-Berastegi G, Sáenz J, Carreno-Madinabetia S, Aristondo O. Future offshore wind energy evolution in the Bay of Biscay. Sustain Energy Technol Assessments 2024;65:103776.

[23] Lavalle C, Gomes CR, Baranzelli C, e Silva FB. Coastal zones. Policy alternatives impacts on European Coastal Zones 2000 – 2050. In: JRC technical notes, Citeseer; 2011.

[24] Butterfield S, Musial W, Jonkman J, Sclavounos P. Engineering challenges for floating offshore wind turbines. Tech. rep., National Renewable Energy Lab.(NREL), Golden, CO (United States); 2007.

[25] Ministerio para la Transición Ecológica y el Reto Demográfico. Plan de ordenación del espacio marítimo. 2023, URL: https://www.miteco.gob.es/es/costas/temas/proteccion-medio-marino/ordenacion-del-espacio-maritimo.html. [Accessed 30 November 2023].

[26] Pérez MG. El plan de ordenación de espacios marítimos de la demarcación marina noratlántica. In: Planificación del espacio marino: Aplicación en España de la Directiva marco 2014/89/UE. RDU; 2022, p. 263–314.

[27] Ministerio de Transportes y Movilidad Sostenible. Visor de la infraestructura de datos espaciales. 2023, URL: http://www.infomar.miteco.es/visor.html. [Accessed 5 November 2024].

[28] Hersbach H, Peubey C, Simmons A, Berrisford P, Poli P, Dee D. ERA-20CM: A twentieth-century atmospheric model ensemble. Q J R Meteorol Soc 2015;141(691):2350–75.

[29] Peuch V-H, Engelen R, Rixen M, Dee D, Flemming J, Suttie M, Ades M, Agustí-Panareda A, Ananasso C, Andersson E, et al. The copernicus atmosphere monitoring service: From research to operations. Bull Am Meteorol Soc 2022;103(12):E2650–68.

[30] Ulazia A, Saenz-Aguirre A, Ibarra-Berastegui G, Sáenz J, Carreno-Madinabeitia S, Esnaola G. Performance variations of wave energy converters due to global long-term wave period change (1900–2010). Energy 2023;268:126632.

[31] Meucci A, Young I, Hemer M, Trenham C. CMIP6 global wind-wave 21st century climate projections phase 1. v13. 2021, Service Collection. URL: http://hdl.handle.net/102.100.100/432508?index=1. [Accessed 5 November 2024].

[32] Meucci A, Young IR, Hemer M, Trenham C, Watterson IG. 140 years of global ocean wind-wave climate derived from CMIP6 access-CM2 and EC-earth3 GCMs: Global trends, regional changes, and future projections. J Clim 2023;36(6):1605–31.

[33] Riahi K, Van Vuuren DP, Kriegler E, Edmonds J, O'neill BC, Fujimori S, Bauer N, Calvin K, Dellink R, Fricko O, et al. The shared socioeconomic pathways and their energy, land use, and greenhouse gas emissions implications: An overview. Glob Environ Chang 2017;42:153–68.

[34] Rusu L. The near future expected wave power in the coastal environment of the Iberian Peninsula. Renew Energy 2022;195:657–69. http://dx.doi.org/10.1016/j.renene.2022.06.047, URL: https://www.sciencedirect.com/science/article/pii/S0960148122008795.

[35] Cannon AJ, Sobie SR, Murdock TQ. Bias correction of GCM precipitation by quantile mapping: how well do methods preserve changes in quantiles and extremes? J Clim 2015;28(17):6938–59.

[36] Carreno-Madinabeitia S, Ibarra-Berastegi G, Sáenz J, Ulazia A. Long-term changes in offshore wind power density and wind turbine capacity factor in the Iberian Peninsula (1900–2010). Energy 2021;226:120364.

[37] Ulazia A, Penalba M, Ibarra-Berastegui G, Ringwood J, Sáenz J. Reduction of the capture width of wave energy converters due to long-term seasonal wave energy trends. Renew Sustain Energy Rev 2019;113:109267.

[38] Penalba M, Kelly T, Ringwood J. Using NEMOH for modelling wave energy converters: A comparative study with WAMIT. 2017.

[39] US Department of Energy. Water power technologies office. 2023, URL: https://www.energy.gov/eere/water/water-power-technologies-office. [Accessed 5 November 2024].

[40] OpenEI. Reference model. 2023, In PRIMRE/Signature Projects. URL: https://openei.org/wiki/PRIMRE/Signature_Projects/Reference_Model. [Accessed 5 November 2024].

[41] Sandia National Laboratories. Reference model project (RMP). 2023, URL: https://energy.sandia.gov/programs/renewable-energy/water-power/projects/reference-model-project-rmp/. [Accessed 5 November 2024].

[42] Laboratory NRE. National renewable energy laboratory. 2023, URL: https://www.nrel.gov/. [Accessed 5 November 2024].

[43] Laboratory PNN. Reference model. 2023, URL: https://tethys-engineering.pnnl.gov/signature-projects/reference-model. [Accessed 5 November 2024].

[44] Laboratory ORN. Oak ridge national laboratory. 2023, URL: https://www.ornl.gov/. [Accessed 5 November 2024].

[45] at Penn State University ARL. Applied research laboratory at penn state university. 2023, URL: https://www.arl.psu.edu/. [Accessed 5 November 2024].

[46] Re-Vision. Re-vision. 2023, URL: https://re-vision.net/. [Accessed 5 November 2024].

[47] Laboratory NRE. Marine energy atlas power matrix analysis. 2023, Retrieved from https://maps.nrel.gov/marine-energy-atlas/power-matrix/analysis. [Accessed 5 November 2024].

[48] Neary VS, Lawson M, Previsic M, Copping A, Hallett KC, Labonte A, Rieks J, Murray D. Methodology for design and economic analysis of marine energy conversion (MEC) technologies. 2014.

[49] Yu Y-H, Jenne D, Thresher R, Copping A, Geerlofs S, Hanna L. Reference model 5 (rm5): Oscillating surge wave energy converter. Tech. rep., National Renewable Energy Lab.(NREL), Golden, CO (United States); 2015.

[50] Bull DL, Smith C, Jenne DS, Jacob P, Copping A, Willits S, Fontaine A, Brefort D, Gordon ME, Copeland R, et al. Reference model 6 (RM6): oscillating wave energy converter. Tech. rep., Sandia National Lab.(SNL-NM), Albuquerque, NM (United States); 2014.

[51] Bull DL, Johnson E. Optimal resistive control strategy for a floating OWC device considering both the oscillating structure and the oscillating water column. Tech. rep., Sandia National Lab.(SNL-NM), Albuquerque, NM (United States); 2013.

[52] Sundar V. Ocean wave mechanics: Applications in marine structures. John Wiley & Sons; 2017.

[53] Cahill B, Lewis T. Wave periods and the calculation of wave power. 2014.

[54] for Medium-Range Weather Forecasts EEC. Parameter database. 2023, Retrieved from https://apps.ecmwf.int/codes/grib/param-db/?id=140112. [Accessed 5 November 2024].

[55] Babarit A. A database of capture width ratio of wave energy converters. Renew Energy 2015;80:610–28.

[56] von Trentini F, Aalbers EE, Fischer EM, Ludwig R. Comparing interannual variability in three regional single-model initial-condition large ensembles (SMILEs) over Europe. Earth Syst Dyn 2020;11(4):1013–31.

[57] for Australian Weather C, Research C, on Forecast Verification Research WJWG. Forecast verification methods. 2015, Retrieved from https://www.cawcr.gov.au/projects/verification/. [Accessed 5 November 2024].

[58] WMO guidelines on the calculation of climate normals. Tech. rep. WMO-No. 1203, Geneva, Switzerland: World Meteorological Organization; 2017, p. 18.

[59] Service CCC. Climate bulletin: Change from 1981–2010 to 1991–2020 reference period (version 08-feb-20). 2023, Retrieved from https://climate.copernicus.eu/sites/default/files/2021-02/C3S_Climate_Bulletin_change_from_1981-2010_to_1991-2020_reference_period_v08-Feb-20_all.pdf. [Accessed 5 November 2024].

[60] Yu Y-H, Li Y, Hallett K, Hotimsky C. Design and analysis for a floating oscillating surge wave energy converter. In: International conference on offshore mechanics and arctic engineering, vol. 45547, American Society of Mechanical Engineers; 2014, V09BT09A048.

[61] AW-Energy. AW-energy - wave energy company. 2023, Retrieved from https://aw-energy.com/. [Accessed 13 November 2024].

[62] Carnegie Clean Energy. CETO technology. 2023, Retrieved from https://www.carnegiece.com/ceto-technology/. [Accessed 13 November 2024].

[63] Biscay Marine Energy Platform (BIMEP). Biscay marine energy platform (BIMEP) official website. 2023, Retrieved from https://www.bimep.com/. [Accessed 13 November 2024].

[64] Wave Hub. Wave hub strengthens position at forefront of wave energy array testing globally. 2014, Retrieved from Web Archive: https://web.archive.org/web/20140728014930/http://www.wavehub.co.uk/news/wave-hub-strengthens-position-at-forefront-of-wave-energy-array-testing-globally/. [Accessed 13 November 2024].
[65] European Marine Energy Centre. European marine energy centre (EMEC). 2023, https://www.emec.org.uk/. [Accessed 13 November 2024].
[66] Torre-Enciso Y, Ortubia I, De Aguileta LL, Marqués J. Mutriku wave power plant: from the thinking out to the reality. In: Proceedings of the 8th European wave and tidal energy conference, uppsala, Sweden, vol. 710, 2009, p. 319–29.
[67] Interreg Europe. BIMEP Mutriku: World's First Breakwater Wave Power Plant & Acceptance of the Community. 2023, Retrieved from https://www.interregeurope.eu/good-practices/bimep-mutriku-worlds-first-breakwater-wave-power-plant-acceptance-of-the-community. [Accessed 13 November 2024].
[68] Jenne DS, Yu Y-H, Neary V. Levelized cost of energy analysis of marine and hydrokinetic reference models. Tech. rep., National Renewable Energy Lab.(NREL), Golden, CO (United States); 2015.
[69] Neary VS, Kobos PH, Jenne DS, Yu Y-H. Levelized cost of energy for marine energy conversion (MEC) technologies. Tech. rep., Sandia National Lab.(SNL-NM), Albuquerque, NM (United States); 2016.
[70] Baca E, Philip RT, Greene D, Battey H. Expert elicitation for wave energy lcoe futures. Tech. rep., National Renewable Energy Lab.(NREL), Golden, CO (United States); 2022.
[71] DeCastro M, Lavidas G, Arguilé-Pérez B, Carracedo P, DeCastro N, Costoya X, Gómez-Gesteira M. Evaluating the economic viability of near-future wave energy development along the Galician coast using LCoE analysis for multiple wave energy devices. J Clean Prod 2024;463:142740.
[72] Ocean Energy Systems (OES). Annual report 2019. 2019, International Energy Agency (IEA) - Ocean Energy Systems (OES). Retrieved from https://www.etipocean.eu/wp-content/uploads/2022/01/200318-oes-annual-report-2019.pdf.
[73] Agency IRE. Wave energy technology brief. 2014, Retrieved from https://www.irena.org/-/media/Files/IRENA/Agency/Publication/2014/Wave-Energy_V4_web.pdf?rev=0b2378736cfc4c1dab1fdf38b0d6d98d. [Accessed 5 November 2024].
[74] Ruiz-Minguela P, Noble DR, Nava V, Pennock S, Blanco JM, Jeffrey H. Estimating future costs of emerging wave energy technologies. Sustainability 2022;15(1):215.
[75] Chang G, Jones CA, Roberts JD, Neary VS. A comprehensive evaluation of factors affecting the levelized cost of wave energy conversion projects. Renew Energy 2018;127:344–54.
[76] Ringwood JV, Zhan S, Faedo N. Empowering wave energy with control technology: Possibilities and pitfalls. Annu Rev Control 2023;55:18–44.
[77] Bacelli G, Ringwood JV. Numerical optimal control of wave energy converters. IEEE Trans Sustain Energy 2014;6(2):294–302.
[78] Arellano-Prieto Y, Chavez-Panduro E, Salvo Rossi P, Finotti F. Energy storage solutions for offshore applications. Energies 2022;15(17):6153.
[79] Gao Q, Bechlenberg A, Jayawardhana B, Ertugrul N, Vakis AI, Ding B. Techno-economic assessment of offshore wind and hybrid wind–wave farms with energy storage systems. Renew Sustain Energy Rev 2024;192:114263.
[80] Nienhuis R, van Rooij M, Prins W, Jayawardhana B, Vakis A. Investigating the efficiency of a novel offshore pumped hydro energy storage system: Experimental study on a scale prototype. J Energy Storage 2023;74:109374.
[81] Bernardino M, Goncalves M, Guedes Soares C. Marine climate projections toward the end of the twenty-first century in the north Atlantic. J Offshore Mech Arct Eng 2021;143(6):061201.
[82] Ibarra-Berastegi G, Ulazia A, Sáenz J, Serras P, Rojí SJG, Esnaola G, Iglesias G. The power flow and the wave energy flux at an operational wave farm: Findings from Mutriku, Bay of Biscay. Ocean Eng 2021;227:108654.
[83] Martinez A, Iglesias G. Mapping of the levelised cost of energy for floating offshore wind in the European Atlantic. Renew Sustain Energy Rev 2022;154:111889.
[84] Ibarra-Berastegui G, Sáenz J, Ulazia A, Sáenz-Aguirre A, Esnaola G. CMIP6 projections for global offshore wind and wave energy production (2015–2100). Sci Rep 2023;13(1):18046. http://dx.doi.org/10.1038/s41598-023-45450-3, Number: 1 Publisher: Nature Publishing Group. URL: https://www.nature.com/articles/s41598-023-45450-3.